Multiple Microstrip Lines on a Multilayered Cylindrical Dielectric Substrate on Perfectly Conducting Wedge

Hesham A. Auda, *Member, IEEE,* and Atef Z. Elsherbeni, *Senior Member, IEEE*

***Abstract*—The quasi-TEM characteristics of a class of cylindrical microstrip lines are rigorously determined. The class of microstrip lines considered consists of multiple infinitesimally thin strips on a multilayered dielectric substrate on a perfectly conducting wedge. Expressions for the potential distribution inside and outside the dielectric substrate, charge distribution on the strips, and capacitance matrix of the microstrip lines are derived. The problems of a microstrip line on a cylindrically capped wedge and on a cylindrical dielectric substrate on perfectly conducting core are also considered as special cases. Sample numerical results based on the derived expressions are given and discussed.**

I. Introduction

PERFECTLY conducting wedges and cylindrically capped wedges are widely utilized in the design of cylindrical radiating structures for aircraft and missiles [1]. A typical radiating structure in such applications consists of a cylindrical–rectangular perfectly conducting patch fed with a microstrip line. In this paper, the quasi-TEM characteristics of a class of cylindrical microstrip lines are rigorously determined. The class of microstrip lines considered consists of multiple infinitesimally thin strips on a multilayered dielectric substrate on a perfectly conducting wedge (see Fig. 1).

The objective of the analysis is to determine the capacitance matrix of the multiconductor transmission line system. The inductance matrix of the multiple microstrips may then be determined, apart from a multiplicative constant, as the inverse of the capacitance matrix that would exist if the multilayered dielectric substrate were replaced by free space [2]. Once the capacitance and inductance matrices are known, the complete behavior of the system can be determined, to the transmission line approximation, by multiconductor transmission line theory [3, ch. 6].

The method of analysis utilized is drawn along the lines of [4]. It relies on the derivation of the exact potential distributions outside and inside the dielectric substrate. The potentials are constructed in such a way that the continuity of the potential, and hence the continuity of the tangential component of the electric field, across the various dielectric interfaces are automatically enforced. Boundary condition equations for the problem are obtained from enforcing the potential to have the specified constant voltages on the strips, and from satisfying the jump discontinuity in the normal derivative of the potential across the dielectric interfaces. These equations are subsequently combined and solved using Galerkin's method. Expressions for the charge distributions on the strips and elements of the capacitance matrix of the microstrip lines are then obtained. The analysis is subsequently specialized to the problems of a microstrip line on a cylindrically capped wedge and on a cylindrical dielectric substrate on a perfectly conducting core (see Fig. 2). Sample numerical results based on the derived expressions are also given and discussed.

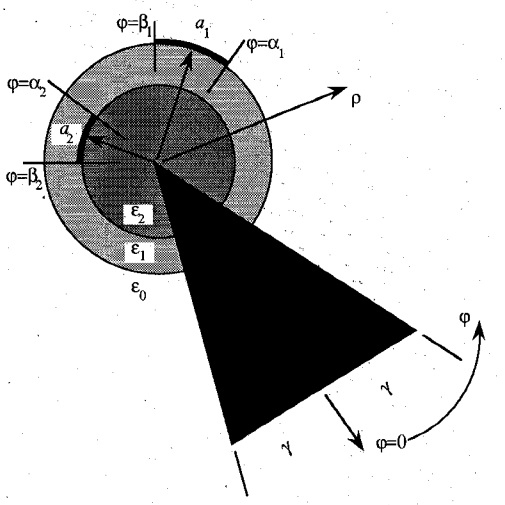

Fig. 1. Multiple microstrip lines on a multilayered cylindrical dielectric substrate on a perfectly conducting wedge.

II. Formulation

In this section, the exact potential distributions outside and inside the mutilayered dielectric substrate are constructed.

The potential in the free space outside the dielectric substrate is constructed such that it satisifes the Laplace equation $\nabla^2 \mathcal{V}_0(\rho,\varphi) = 0, \rho \geq a_1, \gamma \leq \varphi \leq 2\pi - \gamma$, subject to the boundary conditions that $\mathcal{V}_0(a_1,\varphi) = \Phi_1(\varphi), \gamma \leq \varphi \leq 2\pi - \gamma$, and $\mathcal{V}_0(\rho,\gamma) = \mathcal{V}_0(\rho, 2\pi - \gamma) = 0, \rho \geq a_1$. Furthermore, the potential must be both finite and continuous everywhere and regular at infinity. The solution of the Laplace equation in this region can be obtained using the method of separation of

Manuscript received January 21, 1992; revised October 26, 1992.

H. A. Auda is with the Kato Group, 4 Behler Passage, Cairo, Egypt.

A. Z. Elsherbeni is with the Department of Electrical Engineering, University of Mississippi, University, MS 38677.

IEEE Log Number 9208367.

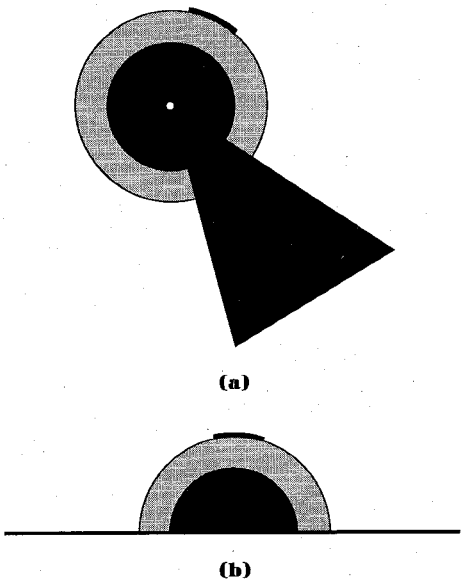

Fig. 2. (a) Microstrip line on a perfectly conducting cylindrically capped wedge. (b) Cylindrical microstrip line on a perfectly conducting cylindrical core.

variables [5, Sect. 4-2] as

$$\mathcal{V}_0(\rho,\varphi) = \sum_{n=1}^{\infty} \nu_n' \left(\frac{a_1}{\rho}\right)^{n\chi(\gamma)} \cdot \sin(n\chi(\gamma)(\varphi-\gamma)) \tag{1}$$

where

$$\nu_n' = \frac{1}{\pi-\gamma}\int_{\gamma}^{2\pi-\gamma} \Phi_1(\varphi) \cdot \sin(n\chi(\gamma)(\varphi-\gamma))\,d\varphi \tag{2}$$

and $\chi(\gamma) = \pi/2(\pi-\gamma)$.

The potential in the outer layer of the dielectric substrate is constructed such that it satisfies the Laplace equation $\nabla^2\mathcal{V}_1(\rho,\varphi) = 0, a_2 \le \rho \le a_1, \gamma \le \varphi \le 2\pi-\gamma$. The boundary conditions on the potential in this layer are as follows: at $\rho = a_1, \mathcal{V}_1(a_1,\varphi) = \Phi_1(\varphi), \gamma \le \varphi \le 2\pi-\gamma$, whereas at $\rho = a_2, \mathcal{V}_2(a_2,\varphi) = \Phi_2(\varphi), \gamma \le \varphi \le 2\pi-\gamma$. Furthermore, $\mathcal{V}_1(\rho,\gamma) = \mathcal{V}_1(\rho,2\pi-\gamma) = 0, a_2 \le \rho \le a_1$. In addition, the potential must be both finite and continuous at all points in the layer and on its boundaries. The solution of the Laplace equation in this layer can likewise be obtained using the method of separation of variables as

$$\mathcal{V}_1(\rho,\varphi) = \sum_{n=1}^{\infty} (\nu_n' F_n(\rho) + \nu_n G_n(\rho)) \sin(n\chi(\gamma)(\varphi-\gamma)) \tag{3}$$

where

$$\nu_n = \frac{1}{\pi-\gamma}\int_{\gamma}^{2\pi-\gamma} \Phi_2(\varphi) \cdot \sin(n\chi(\gamma)(\varphi-\gamma))\,d\varphi \tag{4}$$

and F_n and G_n are functions defined as

$$F_n(\rho) = \frac{1}{R^{2n\chi(\gamma)}-1} \cdot \left(R^{n\chi(\gamma)}\left(\frac{\rho}{a_2}\right)^{n\chi(\gamma)} - \left(\frac{a_1}{\rho}\right)^{n\chi(\gamma)}\right) = \begin{cases} 1, & \rho = a_1 \\ 0, & \rho = a_2 \end{cases} \tag{5}$$

$$G_n(\rho) = \frac{1}{R^{2n\chi(\gamma)}-1} \cdot \left(R^{n\chi(\gamma)}\left(\frac{a_1}{\rho}\right)^{n\chi(\gamma)} - \left(\frac{\rho}{a_2}\right)^{n\chi(\gamma)}\right) = \begin{cases} 0, & \rho = a_1 \\ 1, & \rho = a_2 \end{cases} \tag{6}$$

where $R = a_1/a_2\,(R > 1)$.

Finally, the potential in the inner layer of the dielectric substrate is constructed such that it satisfies the Laplace equation $\nabla^2\mathcal{V}_2(\rho,\varphi) = 0, 0 \le \rho \le a_2, \gamma \le \varphi \le 2\pi-\gamma$, subject to the boundary conditions that $\mathcal{V}_2(a_2,\varphi) = \Phi_2(\varphi), \gamma \le \varphi \le 2\pi-\gamma$, and $\mathcal{V}_2(\rho,\gamma) = \mathcal{V}_2(\rho,2\pi-\gamma) = 0, 0 \le \rho \le a_2$. Furthermore, the potential must be both finite and continuous everywhere, in particular at the origin. Consequently, using the method of separation of variables, $\mathcal{V}_2$ is readily obtained as

$$\mathcal{V}_2(\rho,\varphi) = \sum_{n=1}^{\infty} \nu_n \left(\frac{\rho}{a_2}\right)^{n\chi(\gamma)} \cdot \sin(n\chi(\gamma)(\varphi-\gamma)). \tag{7}$$

III. Equations of the Problem

The potentials outside and inside the dielectric substrate have been constructed in the previous section in such a way that their continuity across the dielectric interfaces, and hence the continuity of the tangential components of the electric field [6, Sect. 3-2], are automatically enforced. There therefore only remains to satisfy the requirement of constant potentials, or zero tangential electric field, at the strips, viz.

$$\Phi_p(\varphi) = V_p, \quad \rho = a_p, \alpha_p \le \varphi \le \beta_p \tag{8}$$

where $p = 1,2$. Furthermore, the normal component of the displacement vector $\boldsymbol{D} = \epsilon\boldsymbol{E} = -\epsilon\nabla\mathcal{V}$ must be discontinuous across each dielectric interface by the amount of the surface free charge density σ on the strip. Thus,

$$\epsilon_{rp}\frac{\partial}{\partial\rho}\mathcal{V}_p(a_p,\varphi) - \epsilon_{r,p-1}\frac{\partial}{\partial\rho}\mathcal{V}_{p-1}(a_p,\varphi) = \begin{cases} \frac{1}{\epsilon_0}\sigma_p(\varphi), & \alpha_p \le \varphi \le \beta_p \\ 0, & \text{otherwise} \end{cases} \tag{9}$$

where $p = 1,2$, and $\epsilon_{r0} = 1$.

IV. Galerkin's Solution

Equation (8) and the last line of (9) are sufficient for the complete evaluation of the potentials Φ_1 and Φ_2 on the dielectric interfaces. A Galerkin's solution of the equations of

the problem can be accomplished by expanding Φ_1 and Φ_2 in terms of a complete set of orthogonal functions on the interval $[\gamma, 2\pi - \gamma]$. The expansion functions need also be chosen so that $\Phi(\gamma) = \Phi(2\pi - \gamma) = 0$. The appropriate expansions of Φ_1 and Φ_2 are therefore

$$\Phi_p(\varphi) = \sum_{k=1}^{\infty} \nu_{pk} \sin(k\chi(\gamma)(\varphi - \gamma)) \tag{10}$$

where $\nu_{pk}, p = 1, 2, k = 1, 2, \cdots$, are real coefficients to be determined.

Substituting (10) into (2) and (4), the coefficients of expansion for the potential distributions are readily found as

$$\nu_k' = \nu_{1k} \tag{11}$$

$$\nu_k = \nu_{2k}. \tag{12}$$

Furthermore, substituting (10), together with (11) and (12), into (8) and the last line of (9), there then results after some simple manipulations the following set of equations.

At $\rho = a_1$:

$$\sum_{k=1}^{\infty} \nu_{1k} \sin(k\chi(\gamma)(\varphi - \gamma)) = V_1, \qquad \alpha_1 \le \varphi \le \beta_1 \tag{13}$$

$$\sum_{k=1}^{\infty} \nu_{1k} k\chi(\gamma)(1 + \epsilon_{r1} R_{1k}) \sin(k\chi(\gamma)(\varphi - \gamma)) - \epsilon_{r1} \sum_{k=1}^{\infty} \nu_{2k} k\chi(\gamma) R_{2k} \sin(k\chi(\gamma)(\varphi - \gamma)) = 0, \qquad \gamma \le \varphi < \alpha_1 \text{ or } \beta_1 < \varphi \le 2\pi - \gamma. \tag{14}$$

At $\rho = a_2$:

$$\sum_{k=1}^{\infty} \nu_{2k} \sin(k\chi(\gamma)(\varphi - \gamma)) = V_2, \qquad \alpha_2 \le \varphi \le \beta_2 \tag{15}$$

$$-\epsilon_{r1} \sum_{k=1}^{\infty} \nu_{1k} k\chi(\gamma) R_{2k} \sin(k\chi(\gamma)(\varphi - \gamma)) + \sum_{k=1}^{\infty} \nu_{2k} k\chi(\gamma)(\epsilon_{r2} + \epsilon_{r1} R_{1k}) \sin(k\chi(\gamma)(\varphi - \gamma)) = 0, \qquad \gamma \le \varphi < \alpha_2 \text{ or } \beta_2 < \varphi \le 2\pi - \gamma \tag{16}$$

where

$$R_{1k} = \frac{R^{2k\chi(\gamma)} + 1}{R^{2k\chi(\gamma)} - 1} \tag{17}$$

$$R_{2k} = 2\frac{R^{k\chi(\gamma)}}{R^{2k\chi(\gamma)} - 1}. \tag{18}$$

Testing the two pairs of equations (13)–(14) and (15)–(16) with $\sin(m\chi(\gamma)(\varphi - \gamma)), m = 1, 2, \cdots$, there finally results the system of algebraic equations

$$\begin{bmatrix} \boldsymbol{X}_{11} & \boldsymbol{X}_{12} \\ \boldsymbol{X}_{21} & \boldsymbol{X}_{22} \end{bmatrix} \begin{bmatrix} \boldsymbol{v}_1 \\ \boldsymbol{v}_2 \end{bmatrix} = \begin{bmatrix} \boldsymbol{V}_1 & \\ & \boldsymbol{V}_2 \end{bmatrix} \begin{bmatrix} \boldsymbol{s}_1 \\ \boldsymbol{s}_2 \end{bmatrix} \tag{19}$$

where the submatrices $\boldsymbol{X}_{11}, \boldsymbol{X}_{12}, \boldsymbol{X}_{21}, \boldsymbol{X}_{22}, \boldsymbol{V}_1$, and $\boldsymbol{V}_2$ of the Galerkin's system of equations are given by

$$\boldsymbol{X}_{11} = [Ss_{mk}(\alpha_1, \beta_1) + k\chi(\gamma)(1 + \epsilon_{r1} R_{1k}) \cdot (Ss_{mk}(\gamma, \alpha_1) + Ss_{mk}(\beta_1, 2\pi - \gamma))] \tag{20}$$

$$\boldsymbol{X}_{12} = [-\epsilon_{r1} k\chi(\gamma) R_{2k} (Ss_{mk}(\gamma, \alpha_1) + Ss_{mk}(\beta_1, 2\pi - \gamma))] \tag{21}$$

$$\boldsymbol{X}_{21} = [-\epsilon_{r1} k\chi(\gamma) R_{2k} (Ss_{mk}(\gamma, \alpha_2) + Ss_{mk}(\beta_2, 2\pi - \gamma))] \tag{22}$$

$$\boldsymbol{X}_{22} = [Ss_{mk}(\alpha_2, \beta_2) + k\chi(\gamma)(\epsilon_{r2} + \epsilon_{r1} R_{1k}) \cdot (Ss_{mk}(\gamma, \alpha_2) + Ss_{mk}(\beta_2, 2\pi - \gamma))] \tag{23}$$

$$\boldsymbol{V}_p = [V_p \delta_{mk}], \qquad p = 1, 2 \tag{24}$$

and the vectors $\boldsymbol{v}_p$ and $\boldsymbol{s}_p, p = 1, 2$, are given by

$$\boldsymbol{v}_p = [\nu_{pk}] \tag{25}$$

$$\boldsymbol{s}_p = [S_m(\alpha_p, \beta_p)]. \tag{26}$$

The functions $S_m(x, y)$ and $Ss_{mk}(x, y)$ denote, respectively, the integrals of $\sin(m\chi(\gamma)(\varphi - \gamma))$ and $\sin(m\chi(\gamma)(\varphi - \gamma)) \sin(k\chi(\gamma)(\varphi - \gamma))$ over the interval $[x, y]$ [4], and δ_{mk} is the Kronecker *delta* function (where $\delta_{mk} = 1$ if $m = k$, and is zero otherwise).

Solution of the system of equations (19) determines the expansion coefficients $\nu_{pk}, p = 1, 2, k = 1, 2, \cdots$, and hence, the complete potential distributions outside and inside the dielectric substrate.

V. Charge Distributios on the Strips and Capacitance Matrix of the Microstrip Line

Substituting $\mathcal{V}_0, \mathcal{V}_1$, and $\mathcal{V}_2$ into the first line of (9), the surface free charge densities on the strips are readily found as

$$\frac{a_1}{\epsilon_0}\sigma_1(\varphi) = \sum_{k=1}^{\infty} \nu_{1k} k\chi(\gamma)(1 + \epsilon_{r1} R_{1k}) \sin(k\chi(\gamma)(\varphi - \gamma)) - \epsilon_{r1} \sum_{k=1}^{\infty} \nu_{2k} k\chi(\gamma) R_{2k} \sin(k\chi(\gamma)(\varphi - \gamma)), \qquad \alpha_1 \le \varphi \le \beta_1 \tag{27}$$

$$\frac{a_2}{\epsilon_0}\sigma_2(\varphi) = -\epsilon_{r1} \sum_{k=1}^{\infty} \nu_{1k} k\chi(\gamma) R_{2k} \sin(k\chi(\gamma)(\varphi - \gamma)) + \sum_{k=1}^{\infty} \nu_{2k} k\chi(\gamma)(\epsilon_{r2} + \epsilon_{r1} R_{1k}) \sin(k\chi(\gamma)(\varphi - \gamma)), \qquad \alpha_2 \le \varphi \le \beta_2 \tag{28}$$

The total charge induced on either strip can now be obtained by integrating the charge density along its corresponding arc length. Thus, integrating both sides of (27) and (28) with respect to φ, respectively, over the intervals $[\alpha_1, \beta_1]$ and

$[\alpha_2, \beta_2]$, the total charges on the strips are given by

$$\frac{1}{\epsilon_0} Q_1(\varphi) = \sum_{k=1}^{\infty} \nu_{1k} k\chi(\gamma)(1 + \epsilon_{r1} R_{1k}) S_k(\alpha_1, \beta_1) - \epsilon_{r1} \sum_{k=1}^{\infty} \nu_{2k} k\chi(\gamma) R_{2k} S_k(\alpha_1, \beta_1) \tag{29}$$

$$\frac{1}{\epsilon_0} Q_2(\varphi) = -\epsilon_{r1} \sum_{k=1}^{\infty} \nu_{1k} k\chi(\gamma) R_{2k} S_k(\alpha_2, \beta_2) + \sum_{k=1}^{\infty} \nu_{2k} k\chi(\gamma)(\epsilon_{r2} + \epsilon_{r1} R_{1k}) S_k(\alpha_2, \beta_2) \tag{30}$$

The total charges Q_1 and Q_2 are related to the strip voltages V_1 and V_2 through the capacitance matrix $\boldsymbol{C} = \epsilon_0[(-)^{i+j} C_{ij}]_{2\times 2}$ according to [5, Sect 3-5]

$$\begin{bmatrix} Q_1 \\ Q_2 \end{bmatrix} = \epsilon_0 \begin{bmatrix} C_{11} & -C_{12} \\ -C_{21} & C_{22} \end{bmatrix} \begin{bmatrix} V_1 \\ V_2 \end{bmatrix}. \tag{31}$$

Apart from the normalization factors $\pm\epsilon_0$, the elements of the capacitance matrix are given by

$$C_{ij} = \left. \frac{Q_i}{V_j} \right|_{V_{l\neq j}=0}, \qquad i, j, l = 1, 2. \tag{32}$$

Consequently, C_{11} and C_{21} can be computed using (29) and (30), where $\nu_{pk}, p = 1, 2, k = 1, 2, \cdots$, are determined by solving the system of equations (19) and $\boldsymbol{V}_2 = 0$. Similarly, C_{12} and C_{22} can be computed using (29) and (30) with $\nu_{pk}, p = 1, 2, k = 1, 2, \cdots$, determined by solving the system of equations (19) with $\boldsymbol{V}_1 = 0$.

VI. Alternative Expressions for the Line Capacitances

An alternative set of more explicit, although less direct, expressions for the elements of the capacitance matrix is given in this section. The new expressions are arrived at by expanding Φ_1 and Φ_2 in the form

$$\tilde{\Phi}_p(\varphi) = V_p \sum_{k=1}^{\infty} \tilde{\nu}_{pk} \sin\left(k\chi(\gamma)(\varphi - \gamma)\right) \tag{33}$$

where $p = 1, 2$, rather than as in (10). The result of this simple modification is a Galerkin's system of equations similar to (19), except that the new vectors of coefficients $\boldsymbol{v}_1$ and $\boldsymbol{v}_2$ are postmultiplied with $\boldsymbol{V}_1$ and $\boldsymbol{V}_2$, respectively. In this case, the new vectors of coefficients are solved for under the conditions $V_1 = V_2 = 1$ (even mode excitation) and $V_1 = -V_2 = 1$ (odd mode excitation). Using the potential expansion (33) to obtain the charge distributions on the strips, then integrating the derived charge distributions over the lengths of the corresponding strips, a matrix relationship for the applied voltages and total charges induced on the strips similar to (31) is obtained. The elements of the modified capacitance matrix are then given by

$$\tilde{C}_{11} = \sum_{k=1}^{\infty} \tilde{\nu}_{1k} k\chi(\gamma) \cdot (1 + \epsilon_{r1} R_{1k}) S_k(\alpha_1, \beta_1) \tag{34}$$

$$\tilde{C}_{21} = 2\epsilon_{r1} \sum_{k=1}^{\infty} \tilde{\nu}_{2k} k\chi(\gamma) \cdot R_{2k} S_k(\alpha_1, \beta_1) \tag{35}$$

$$\tilde{C}_{12} = 2\epsilon_{r1} \sum_{k=1}^{\infty} \tilde{\nu}_{1k} k\chi(\gamma) \cdot R_{2k} S_k(\alpha_2, \beta_2) \tag{36}$$

$$\tilde{C}_{22} = \sum_{k=1}^{\infty} \tilde{\nu}_{2k} k\chi(\gamma) \cdot (\epsilon_{r2} + \epsilon_{r1} R_{1k}) S_k(\alpha_2, \beta_2). \tag{37}$$

Because of the linearity of the multiple microstrip line system, the original and modified line capacitances are related according to

$$C_{ij} = \tfrac{1}{2}(\tilde{C}_{ij}|_{V_1=V_2=1} + (-)^{j-1} \tilde{C}_{ij}|_{V_1=-V_2=1}), \qquad i, j = 1, 2. \tag{38}$$

VII. Microstrip Line on a Cylindrically Capped Wedge and the Cylindrical Microstrip Line

The previous analysis is readily specialized to the problem of a microstrip line on a cylindrically capped wedge. In this case, the inner strip is extended to cover the whole inner dielectric interface. Thus, setting $\alpha_2 = \gamma$ and $\beta_2 = 2\pi - \gamma$, there results $\boldsymbol{X}_{21} = 0, \boldsymbol{X}_{22} = [(\pi - \gamma)\delta_{mk}]$, and $\boldsymbol{s}_2 = 0$. It then follows that $\boldsymbol{v}_2 = 0$, and hence, $\Phi_2 = 0$, as should have been expected. The Galerkin's system of equations then reduces to

$$\boldsymbol{X}_{11} \boldsymbol{v}_1 = \boldsymbol{s}_1 \tag{39}$$

where the multiplication factor V_1 is suppressed from the right-hand side for convenience. Solution of the system of equations (39) determines the expansion coefficients $\nu_{1k}, k = 1, 2, \cdots$, and hence, the complete potential distributions outside and inside the dielectric substrate. The charge distribution on the strip and capacitance of the microstrip line are then given by

$$\frac{a_1}{\epsilon_0} \sigma(\varphi) = \sum_{k=1}^{\infty} \nu_{1k} k\chi(\gamma)(1 + \epsilon_{r1} R_{1k}) \cdot \sin(k\chi(\gamma)(\varphi - \gamma)) \tag{40}$$

$$C = \epsilon_0 \sum_{k=1}^{\infty} \nu_{1k} k\chi(\gamma)(1 + \epsilon_{r1} R_{1k}) \cdot S_k(\alpha_1, \beta_1). \tag{41}$$

Another important cylindrical microstrip line that can be considered as a special case is the cylindrical microstrip line on a cylindrical dielectric substrate on perfectly conducting core [7], [8]. This is the case when the wedge angle for the cylindrically capped wedge is equal to π. The charge distribution on the strip and capacitance of the microstrip line in this case are equal to one half the charge distribution and capacitance given by (40) and (41), where the coefficients of

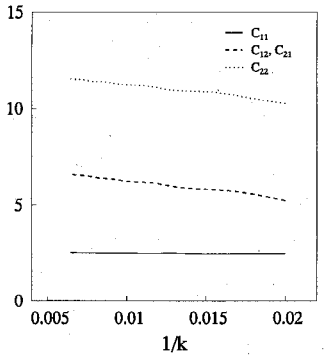

Fig. 3. Convergence of line capacitances for multiple microstrip lines on a multilayered cylindrical dielectric substrate on a perfectly conducting wedge ($R = 1.5, \gamma = 45°, \epsilon_{r1} = 4.7$, and $\epsilon_{r2} = 12$): $\alpha_{1,2} = 167.5°$ and $\beta_{1,2} = 192.5°$.

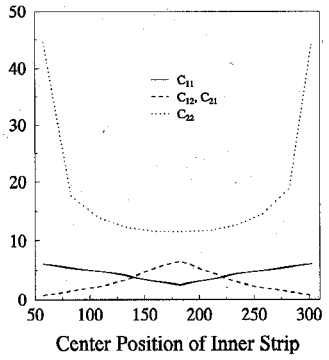

Fig. 4. Line capacitances for the same multiple microstrip line configuration in Fig. 3 as the inner strip ($\beta_2 - \alpha_2 = 25°$) changes position while an identical strip is placed on the outer boundary at $\alpha_1 = 167.5°$ and $\beta_1 = 192.5°$.

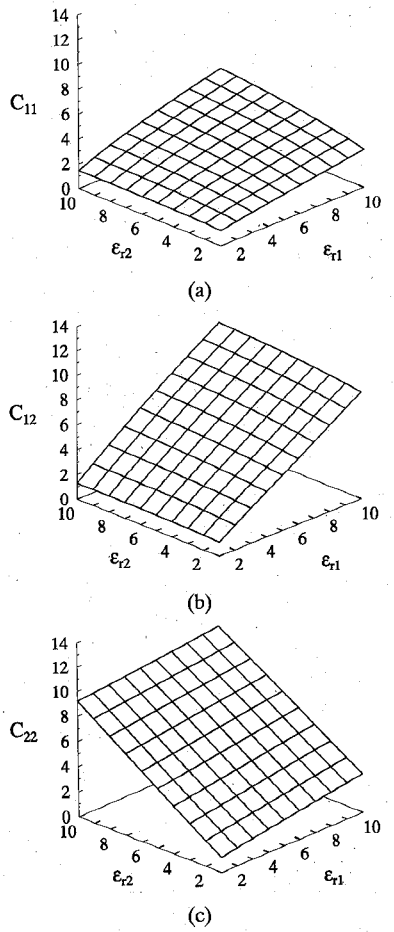

Fig. 5. Line capacitance surfaces $C_{ij}(\epsilon_{r1}, \epsilon_{r2}), i, j = 1, 2$ for 25°-wide, edge-coupled strips ($\alpha_1 = 155°, \beta_1 = 180° = \alpha_2$, and $\beta_2 = 205°$): $R = 1.5$ and $\gamma = 45°$.

expansion $\nu_{1k}, k = 1, 2, \cdots$, are obtained by solving (39) with $\gamma = \pi/2$ and $\chi(\gamma) = 1$

VIII. Numerical Results and Discussions

The analysis in the paper has been implemented as a Fortran program. The potential distributions on the dielectric interfaces, charge distributions on the strips, and capacitance matrix of the microstrip lines have been computed for both the wedge and cylindrically capped wedge geometries for a wide variety of parameter values.

Insight into the convergence characteristics of the solution can be gained by considering the alternative set of expressions for the line capacitances given in Section VI. Examination of (17) and (18) shows that R_{1k} tends (decreases) to "1," and hence R_{2k} tends to zero, monotonically as k tends to infinity. Furthermore, it can be shown that, for any given $N, R_{1K} \leq 1 + 10^{-N}$, and hence, $R_{2,2K} \leq 10^{-N}$, where K is an integer given by

$$K = \left[\left(1 - \frac{\gamma}{\pi}\right)\frac{\log_{10}(1 + 10^{N+\log_{10}(2)}}{\log_{10}(R)}\right], \quad \gamma < \pi, R > 1 \tag{42}$$

where $[x]$ denotes the smallest integer greater than or equal to x. For large N, say $N = 7$, then $K = [N/(2\chi(\gamma)\log_{10}(R))]$. Inspection of the linear graph $G(K, \gamma)$ given by (42) shows that the number of terms K decreases as either R or γ is increased. As an example, let $\gamma = 45°$ and $N = 7$. Hence, it follows from (42) that $K = 16$ for $R = 1.5$ and $K = 67$ for $R = 1.1$. It should be pointed out that this does not necessarily imply that convergence is achieved after only $2K$ terms since the coefficients of expansion obtained by solving the matrix equation (19), modified in the manner indicated in Section VI, need not have actually converged after only so many terms. In fact, since $|k\chi(\gamma)S_k(\alpha_p, \beta_p)| = |\cos(k\chi(\gamma)(\alpha_p - \gamma)) - \cos(k\chi(\gamma)(\beta_p - \gamma))| \leq 2, p = 1, 2$, convergence of the line capacitances is assured with the convergence of $\tilde{\Phi}_1$ and $\tilde{\Phi}_2$. Since $\tilde{\nu}_{pk}, p = 1, 2$ are coefficients for Fourier series, then $\tilde{\nu}_{pk} = O(1/k^\theta), \theta > 1$ as k tends to infinity, i.e., there exists an integer L and a constant A such that $|\tilde{\nu}_{pk}| \leq A/k^\theta$ for all $k \geq L$ [9, Sect. 5-8]. Simple algebra then shows that the tail end terms ($k \geq \max(2K, L)$) of the series for $\tilde{C}_{21}$ and $\tilde{C}_{12}$ are bounded by $4A\epsilon_{r1}R^{-}k\chi(\gamma))/k^\theta$. The bounds for the terms of the series for $\tilde{C}_{11}$ and $\tilde{C}_{22}$ are, respectively, $2A(1 + \epsilon_{r1})/k^\theta, 2A(\epsilon_{r2} + \epsilon_{r1})/k^\theta, k \geq \max(K, L)$. As can be seen, the rate of convergence improves as R is increased. This is readily attributed to the fact that coupling between the

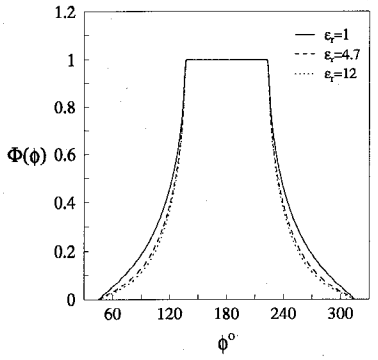

Fig. 6. Potential distribution on the free space–dielectric interface of a microstrip line on a cylindrically capped wedge ($R = 2, \gamma = 45°, \alpha_1 = 135°$, and $\beta_1 = 225°$).

strips decreases as R is increased, so that a fewer number of terms would be needed to represent a weaker field in the outer layer of the dielectric substrate. The rate of convergence also improves as the strips become wider because of the pulse-like waveforms of $\tilde{\Phi}_1$ and $\tilde{\Phi}_2$ [4].

The convergence patterns for the line capacitances of multiple microstrip lines on a multilayered dielectric substrate on wedge ($R = 1.5, \gamma = 45°, \epsilon_{r1} = 4.7$, and $\epsilon_{r2} = 12$) are shown in Fig. 3 under conditions of maximum coupling, i.e., $\alpha_1 = \alpha_2 (= 167.5°)$ and β_1 and $\beta_2 (= 192.5°)$. The line capacitances for the same multiple microstrip line configuration are plotted in Fig. 4 as the inner strip ($\beta_2 - \alpha_2 = 25°$) is moved while the position of the outer strip is kept constant. Furthermore, the three-dimensional line capacitance surfaces $C_{ij}(\epsilon_{r1}, \epsilon_{r2}), i, j = 1, 2$ are shown in Fig. 5 for $R = 1.5$ and $\gamma = 45°$ in the case of 25°-wide, edge-coupled strips ($\alpha_1 = 155°, \beta_1 = 180° = \alpha_2$, and $\beta_2 = 205°$). The surfaces are clearly planar. Finally, the potential distributions on the free space–dielectric interface of a microstrip line on a cylindrically capped wedge ($R = 2, \gamma = 45°, \alpha_1 = 135°$, and $\beta_1 = 225°$) are shown in Fig. 6 for different dielectric constants ϵ_{r1}, whereas the three-dimensional effective dielectric constant surfaces $\epsilon_{r\text{eff}}(\epsilon_{r1}, R) = C_1(\epsilon_{r1}, R)/C_1(\epsilon_{r1} = 1, R)$ for a microstrip line symmetrically located on a cylindrically capped wedge are shown in Fig 7 for different strip widths. Apart from values of R close to unity, the effective dielectric constant surfaces are planar. Thus, the sensitivity of the normalized propagation constant (characteristic impedance) with respect to changes of the substrate's dielectric constant or R is a bounded monotonically increasing (decreasing) function of the dielectric constant or R [4].

IX. Summary

The quasi-TEM characteristics of a class of cylindrical microstrip lines have been rigorously determined in this paper. The class of microstrip lines considered consists of multiple infinitesimally thin strips on a multilayered dielectric substrate on a perfectly conducting wedge. Expressions for the potential distribution inside and outside the dielectric substrate, charge distribution on the strips, and capacitance matrix of the microstrip lines have been derived. The analysis has then been specialized to the problems of a microstrip line on a cylindrically capped wedge and on a cylindrical dielectric substrate on a perfectly conducting core. Sample numerical results based on the derived expressions have also been given and discussed.

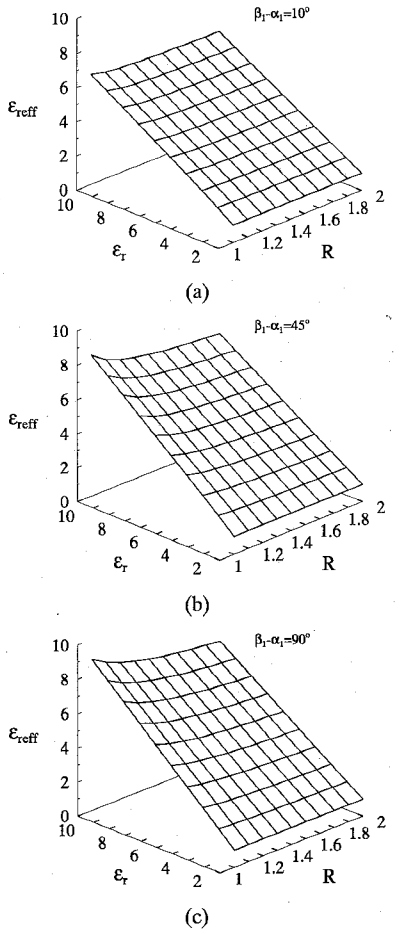

Fig. 7. Effective dielectric constant surfaces $\epsilon_{r\text{eff}}(\epsilon_{r1}, R) = C_1(\epsilon_{r1}, R)/C_1(\epsilon_{r1} = 1, R)$ for a symmetrical microstrip line on a cylindrically capped wedge for different strip widths: $\gamma = 45°$.

References

[1] J. R. Wait, *Electromagnetic Radiation from Cylindrical Structures.* Elmsford, NY: Pergamon, 1959.
[2] C. Wei, R. F. Harrington, J. R. Mautz, and T. K. Sarkar, "Multiconductor transmission lines in multilayered dielectric media," *IEEE Trans. Microwave Theory Tech.*, vol. MTT-32, pp. 439–450, Apr. 1984.
[3] D. Kajfez, *Notes on Microwave Circuits.* Oxford, MS: Kajfez Consulting, 1986.
[4] H. A. Auda, "Cylindrical microstrip line partially embedded in a perfectly conducting ground plane," *IEEE Trans. Microwave Theory Tech.*, vol. 39, pp. 1662–1666, Sept. 1991.
[5] R. Plonsey and R. E. Collin, *Principles and Applications of Electromagnetic Fields.* New York: McGraw-Hill, 1961.
[6] J. A. Stratton, *Electromagnetic Theory.* New York: McGraw-Hill, 1941.
[7] N. G. Alexopoulos and A. Nakatani, "Cylindrical substrate microstrip line characterization," *IEEE Trans. Microwave Theory Tech.*, vol. MTT-35, pp. 843–849, Sept. 1987.
[8] D. Homentcovschi, "A cylindrical multiconductor stripline-like microstrip transmission line," *IEEE Trans. Microwave Theory Tech.*, vol. 37, pp. 497–503, Mar. 1989.
[9] G. P. Tolstov, *Fourier Series.* New York: Dover, 1962.

Hesham A. Auda (S'82–M'84) was born in Cairo, Egypt, on February 5, 1956. He received the B.Sc. degree from Cairo University, Cairo, Egypt, in 1978, the M.Eng. degree from McGill University, Montreal, Canada, in 1981, and the Ph.D. degree from Syracuse University, Syracuse, NY, in 1984, all in electrical engineering.

In 1984 he joined the University of Mississippi, University, as an Assistant Professor of Electrical Engineering, and was promoted to the Associate Professor rank in 1989. In 1990, he joined Kato Group, Cairo, Egypt, as an Assistant to the Chairman of the Board. His areas of interest include microwave circuits, antennas, and the mathematical and numerical solution of electromagnetic field problems.

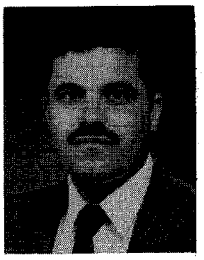

Atef Z. Elsherbeni (M'86–SM'91) was born in Cairo, Egypt, on January 8, 1954. He received the B.Sc. (Honors) degree in electronics and communication, the B.Sc. (Honors) degree in applied physics, and the M.Eng. degree in electrical engineering, all from Cairo University, Cairo, Egypt, in 1976, 1979, and 1982, respectively, and the Ph.D. degree in electrical engineering from Manitoba University, Winnipeg, Man., Canada, in 1987.

He was a Research Assistant with the faculty of Engineering at Cairo University from 1967 to 1982, and at the Department of Electrical Engineering, Manitoba University from 1983 to 1986. After receiving the Ph.D. degree, he became a Post-Doctoral Fellow at the same department, and later joined the faculty of the University of Mississippi in August 1987, where he is now an Associate Professor of Electrical Engineering. His areas of professional interest include the scattering and diffraction of electromagnetic waves, numerical techniques, antennas, and computer-aided design. He has authored/coauthored over 90 technical papers and reports on applied electromagnetics, antenna design, and other subjects of microwave engineering.

Dr. Elsherbeni is a member of the IEEE Antennas and Propagation and Microwave Theory and Techniques Societies, and is an honorary member of the Electromagnetics Academy and Sigma Xi.